Potential applications for image-based systems in structural engineering

O. De La Torre,[1,3,4] S. Newell,[1,2] M.H. Flanagan,[1,5] J. Goggins,[1,3,4]
[1]Civil Engineering, National University of Ireland Galway, University Road, Galway, Ireland
[2]Galway-Mayo Institute of Technology, Old Dublin Road, Galway, Ireland
[3]Centre for Marine and Renewable Energy Ireland (MaREI), Galway, Ireland
[4]Ryan Institute, National University of Ireland, Galway, Ireland
[5]EireComposites Teo, Indreabhan, Galway, Ireland
emails: oscar.delatorre@nuigalway.ie, s.newell2@nuigalway.ie, m.flanagan15@nuigalway.ie, jamie.goggins@nuigalway.ie

ABSTRACT: This paper presents a series of examples where systems based on images have been used to quantify deformation and strain fields for different applications. The objective of this work is to highlight the strengths and weaknesses of these technologies compared to more traditional systems. In particular, two image-based technologies have been studied: a Digital Image Correlation (DIC) device and a high speed camera. The former has been used in three different static tests: a compression test, a 4 points bending test and a tensile test. The latter was employed in a vibration analysis where the DIC could not be used due to its particular camera specification. Both technologies potentially produce easy to interpret results, which with commonly used alternative technologies usually require a significant post process effort. On the other hand, for effective and reliable results, the image-based technologies can require a previous treatment of the sample and a very careful experimental setup. Moreover, the possibility of performing global measurements compared to more local ones carried out by conventional sensors make these systems very attractive for structural engineering.

KEY WORDS: Digital Image Correlation, High Speed Acquisition, Speckle

1 INTRODUCTION

Image based technologies have been extensively used in many fields of science for a long time now (for example, medicine, space, physics). In the recent years, the significant improvement in cameras performance (for example, resolution, rate, sensors) and reduction in cost has made these technologies accessible and suitable for monitoring a large variety of structural engineering applications. The aim of the present paper is to show different applications where image based technologies have been used and evaluate not only their results, but also the experimental setup and post process data flow required to obtain them.

Digital Image Correlation (DIC) is a non-contact optical method based on full field speckle images which can be used to measure displacement and/or strain [1]. It basically takes pictures at different stages of deformation or movement and by tracking subsets of pixels it can correlate the displacement and/or the strain between different images [2],[3]. Stereo images using two or more cameras can produce 2D and also 3D results.

High speed image acquisition works under exactly the same principle as normal acquisition, but by dramatically reducing the exposure time, frequencies of several thousands of frames per second are currently easily achieved [4]. Such high frequencies could be useful to observe sudden phenomena or high frequency vibration [5].

2 TESTED CASES

In order to gain knowledge of the strengths and weaknesses of these technologies, a variety of tests have been designed. Compression, bending and tensile tests have been performed with samples of very different shapes and materials. Specifically, DIC was employed in the following tests (i) a carbon fiber cylinder statically compressed to observe its buckling performance, (ii) a 3.65 meters long precast concrete slab in a four points bending test to check its deflection and (iii) a glass fibre epoxy sample in a classic tension test. Also, a high speed camera has been used to characterise a modal test table in terms of its frequency-displacement performance.

Figure 1. Some of the tested objects: a carbon fibre cylinder (top tight), shaker (top left) and concrete slab/planck (bottom)

2.1 DIC tests setup

An ARAMIS 5M (GOM ®) model has been used for this work. It is a stereo camera device (2448 x 2050 pixel resolution) with 12 mm focal length lens. Before proceeding with the actual test, in order to use DIC technology, the tested

sample should be prepared. The images used should be grey-scaled and with a high level of contrast. As explained above, DIC tracks subsets or facets between images at different levels of strain or displacement. These facets typically undergo displacement and deformation so any point of the facet could change its relative position to another from image to image. In order to be able to locate them among the images there should be a system to reference them. Assuming a very simple system where a single facet (center point A and generic point B) is displaced and deformed between time t and time t+δt, we should consider the quantities shown in Figure 2.

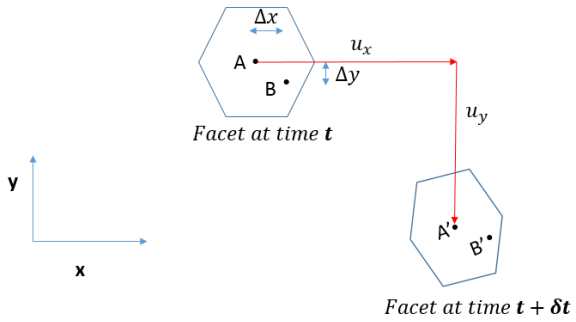

Figure 2. Facets movement and deformation.

As observed, the facet at time t+δt has been displaced (the center of the facet has moved from A to A') and deformed (distance AB is different than distance A'B') with respect to time t. Equation (1) and (2) let us relate the centre location of the facet at both instants of time:

$$x' = x + u_x + \frac{\delta u_x}{\delta x}\Delta x + \frac{\delta u_y}{\delta y}\Delta y \quad (1)$$

$$y' = y + u_y + \frac{\delta u_y}{\delta x}\Delta x + \frac{\delta u_x}{\delta y}\Delta y \quad (2)$$

The displacement field is obtained from the A to A' movement and the strain field from the partial derivatives in the equations.

A speckle pattern is frequently applied on the sample's surface under study. In order to increase the contrast, a white paint layer is usually applied beforehand. Figure 3 shows the samples used in this work with their respective speckle pattern.

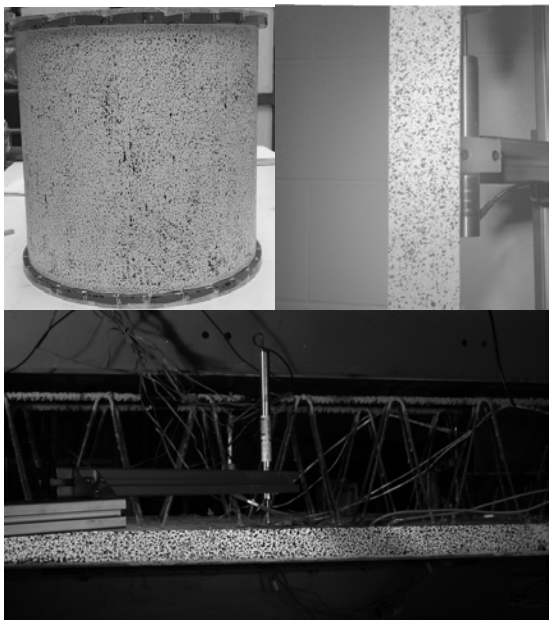

Figure 3. Speckle patterns on the tested samples.(a) Composite cylinder for compression test, (b) GRFP coupon for tensile test, and (c) precast concrete filigree slab for bending test

Equations (1) and (2) clearly address a major issue related to DIC: results depend on how well identified the points are in each image. This means that ultimately, the results are speckle dependant. There is a significant amount of literature studying the effects of pattern quality, type, speckle size and/or subset size on the obtained results, [6], [7], [8]. This leads to very careful and time consuming test setups going through an iterative process to evaluate the speckle pattern itself. In this work, three different field of views have been used for the DIC cameras: 300 x 250 mm^2 for the tensile test, 750 x 600 mm^2 for the cylinder test and 1000 x 800 mm^2 for the concrete slab. Since the speckle size is related to the field of view two different methods have been used to produce the desired speckle patterns: a spray for the glass fibre test and a pattern brush for the bigger areas. It is important to mention that the accuracy of the results is obviously related to the chosen field of view (typically given as a % of the FOV) and, therefore should be previously taken into account.

2.2 Glass fiber sample tension test

A 50 mm wide and 340 mm long glass fibre reinforced composite sample has been tested. The layup of the glass was [(+/-45),0]s and it was tested normal to the 0 fibres in order to observe as much strain as possible. A 5 mm/min displacement controlled loading rate has been used during the tensile test. A 1 Hz sampling frequency has been used for the DIC and a 300 x 250 mm^2 field of view. In order to check the accuracy of the DIC capturing local strain effects, a strain gauge has been also installed. Figure 4 shows the sequence of the test.

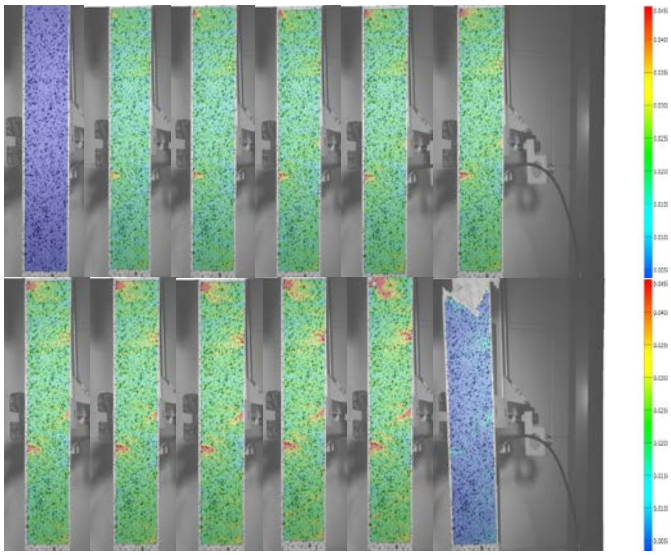

Figure 4. Strain field, in microstrain, within the sample during the test

The strain field within the sample can be considered as a rather homogenous field where very important local tensions develop. These strain concentrations indicate sub surface defects and, hence, DIC could be used as a non-destructive test technique for composites. Ultimately one of these local phenomena produces the failure, but these plots are extremely useful to conclude that there are other zones in the sample of high failure risk.

In order to analyse local strains a virtual area has been simulated on the sample's surface which approximately corresponds to the strain gauge location (on the opposite face), as shown in Figure 5.

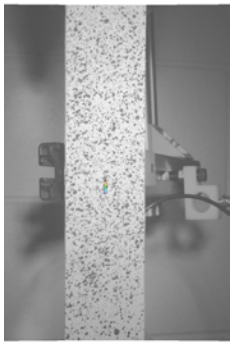

Figure 5. Strain Gauge analogous region.

The results comparison before failure are shown in Figure 6. The DIC seems to capture to a good agreement the behaviour of the strain gauge. The results in the virtual area have been averaged for all the images, which could explain the smoother profile of the DIC results.

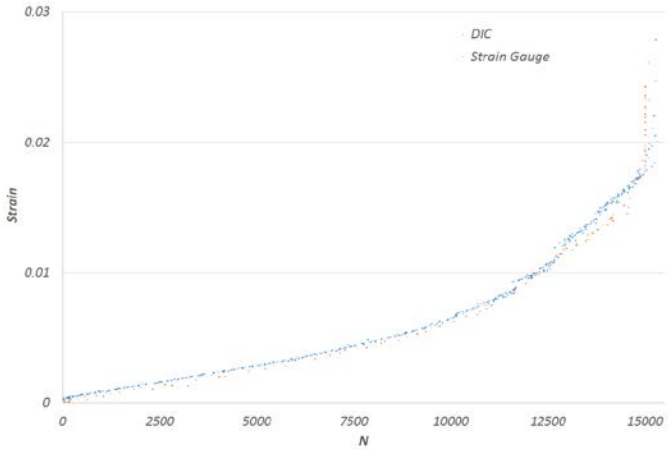

Figure 6. Averaged DIC strain results in the region (orange) and strain gauge results (blue) versus load for a standardised tensile coupon test

2.3 Cylinder buckling test

A 500 mm height cylinder has been compressed to analyse its buckling pattern. Its diameter tappers from 531.4 mm (top side) to 544.5 mm (bottom side) and it is made of carbon fiber. A 5kN loading step has been used and photographs have been taken in every step until failure. A 750 x 600 mm^2 field of view has been used, which effectively covered the whole height of the sample. Figure 7 shows the cylinder before and after failure within the test rig. In the rightmost image, a horizontal displacement field calculated by the DIC has been overlapped.

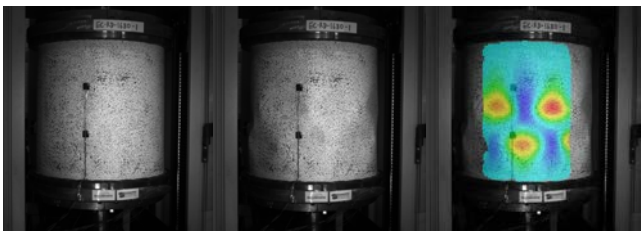

Figure 7. Before (left) and after (center) images of the tested cylinder. Resulting displacement field overlapped (right)

Even if, in this case, the buckling shape is clearly visible to the naked eye, given the resulting displacement levels, obtaining field results along an area could make further analysis easier. For instance, in this case 5 different sections have been defined equidistantly spaced and perpendicular to the cylinder axis as shown in Figure 8. Displacement along the different sections can be then plotted to better study the resulting diamond shape pattern.

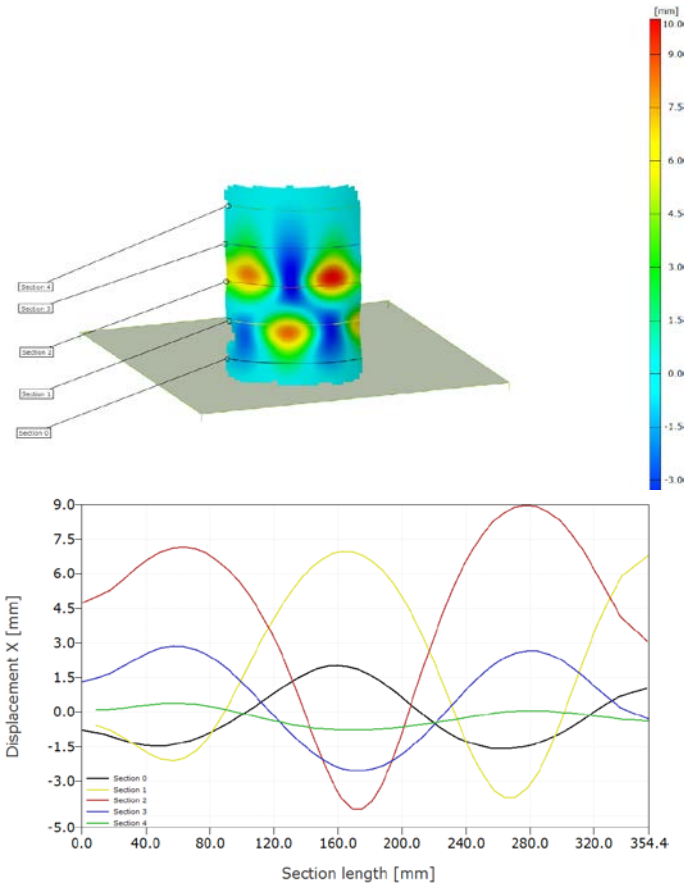

Figure 8. General 3D results (top) and displacement along the different sections (bottom)

2.4 Four points bending concrete slab

A 3.65m long x 0.55m wide x 0.065 m thick precast concrete lattice girder plank has been tested in a 4 points bending configuration (lower image Figure 1). The slab has been loaded by means of a hydraulic actuator, which was moving at a rate of 0.6 mm/min until failure. In order to observe the deflections between the two loading points, the DIC was positioned adjacent to the side of the plank with a 1000x800 mm^2 field of view such that the full thickness of the plank was observed. An image every 30 seconds has been acquired. A Linear Variable Differential Transformer (LVDT) sensor has been located at midspan which was also observable using the DIC (Figure 3). The LVDT measures in the vertical direction and has been used to compare with DIC results. A comparison of the vertical deflection measured by the DIC and LVDT is shown in Figure 9. Since the LVDT position can be clearly identified using the DIC, a virtual point has been located in the equivalent location. The recorded data from the LVDT is compared with this equivalent point in Figure 9.

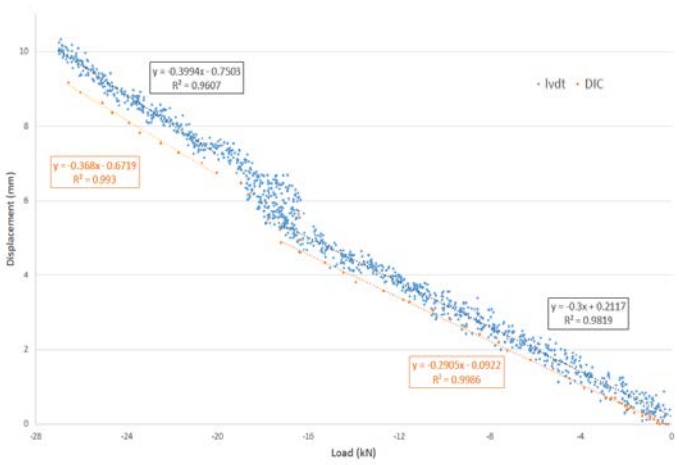

Figure 9. LVDT results (blue) and DIC results (orange) of the equivalent point

As observed in Figure 9, the DIC follows the trend shown by the LVDT's results. During the test, there was a sudden movement of the reaction frame where the actuator is attached and that is clearly visible in both results (around 17 kN). After this, the DIC results are well below the LVDT. Since the LVDT is a single-point contact sensor, it is very likely that after the sudden movement of the frame, the sensor is measuring a different point and given the surface roughness of the concrete sample the gap between the DIC and the LVDT results can increase as shown in the last part of the loading. This could also be the cause of the important dispersion of the LVDT's results. DIC seems, though, to typically predict lower displacements over the entire range of loading. The trend lines shown in Figure 9 for both 0 to 17 kN and 20 to 26 kN ranges highlight the difference.

When observing the field displacement along the whole measured area of the precast plank, the unsymmetrical deformation of the precast plank was noted. In Figure 10, the vertical displacement as recorded by the DIC is shown and highlights the deformation pattern of the plank at midspan. As observed, the load was not equally applied at both sections and, therefore, the slab was more deflected on one extreme (right side of the image) than the other (left side of the image).

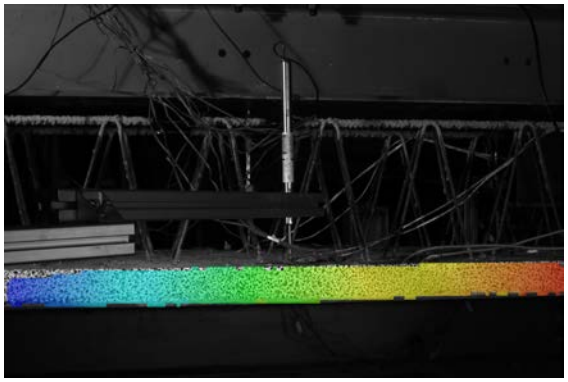

Figure 10. Vertical displacement field results indicating non-symmetrical deformation

2.5 *High speed camera test setup*

Due to the current specifications of the cameras in this DIC device, it is not possible to use it to analyze high frequency phenomena. Whenever the exposure time of the photograph is of the same order of magnitude as the time scale of the phenomenon to be captured, the results are not reliable. Therefore, to analyze the vibration performance of a shaker (Figure 1) in the 20-1000 Hz range a high speed camera has been used.

Since several thousands of frames per second (fps) are typically acquired with these cameras, it is necessary to use a good lighting system that allows the sensor capturing the sample. For this test, a Vision Research Phantom v310 camera has been used along with two Dedocool tungsten light heads. This camera can record at 3250 fps at a full resolution (1280 x 800), but higher rates can be achieved by decreasing the resolution.

2.6 *Frequency-displacement performance test*

The objective of this test is to study the peak to peak travel of the shaker at full power (±5 V) for different frequencies. In order to compare the results obtained by analyzing the images, an accelerometer (ENDEVCO 752A12) has been located on the top of the M6 thread by means of a magnet (Figure 11). Six different frequencies have been studied. The camera has recorded at 5600 fps for all of the cases. The image resolution is 800 x 600.

Figure 11. ENDEVCO 752A12 accelerometer with a magnet base.

In order to post process the images and accelerometer's data, a Labview programme developed in-house has been used. Figure 12 shows a Labview capture of the edge identification used to measure the effective displacement of the sample in the vertical direction.

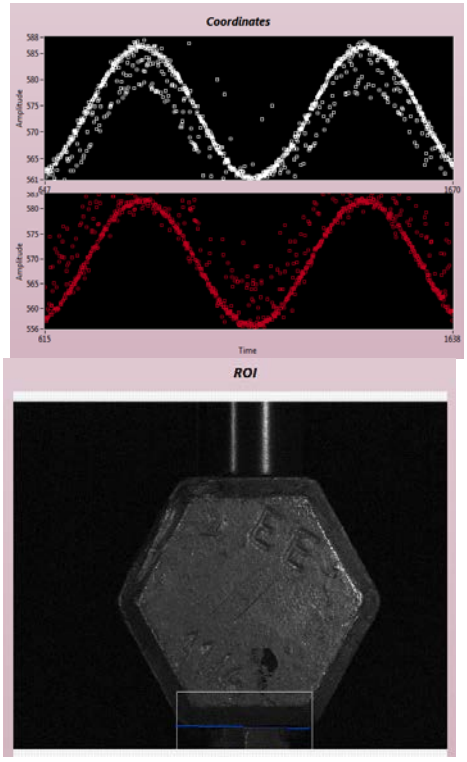

Figure 12. Postprocessing routine capture. Vertical coordinates plot (top) and Region of Interest under study (bottom)

In order to check the double integration procedure required to obtain the displacement from the accelerometer's output, a previous comparison between the accelerometer and a LVDT has been done at 10 Hz and 2V and at 20 Hz and 5V. When integrating, the low frequency band is amplified and a filter is necessary to avoid non desired frequencies. In this case, a highpass filter has been used with a cutoff frequency of 95% of the exciting frequency. Table 1 shows this comparison and the relative error, equation (3), where the LVDT result has been used as the reference value.

$$e = \left| \frac{x_i - x_{ref}}{x_{ref}} \right| \cdot 100 \quad (3)$$

where x_{ref} is the reference value.

Table 1. Peak to peak displacement (mm) comparison between the accelerometer and the LVDT

Frequency (Hz)	10	20
Voltage (V)	2	5
LVDT	2.3	5.4
	86	77
Accelerometer	2.3	5.3
	47	22
Error (%)	1.6	2.8

Table 2 summarises the obtained results both by double integrating the accelerometer's signal and by image identification for the six different tested frequencies

Table 2. Peak to peak displacement (mm) for the different tested frequencies

Frequency (Hz)	20	40	80	100	200	500
Accelerometer	5.322	5.680	1.439	0.772	0.130	0.017
High Speed Camera	7.068	7.400	1.814	0.982	0.123	---
Error (%)	32.8	30.3	26.1	27.2	5.4	---

There is a significant level of noise in the coordinates detection (Figure 12), which suggests that a better focus of the edges of the surface should have been done. During the test, the focus has been manually adjusted for every case. A poor focus of the region of interest leads to higher errors as clearly shown in Table 2. Moreover, the images used give a ratio of approximately 0.123 mm/pixel, which is clearly insufficient to capture the vibration at 500 Hz.

3 CONCLUSIONS

Image based technologies can be a reliable solution for quantifying phenomenon of different structural problems, as shown in the present work. These systems output non-contact measurements and field (multiple points) measurements which can be of great value depending on the application. When compared to more traditional, local and contact sensors their results are in good agreement.

DIC on the other hand, requires a sample preparation which can be both challenging and very time consuming. Also, a certain level of expertise should be gained to avoid speckle dependent results.

High speed imagery postprocessing is not simple and even with flexible programming tools such as Labview, the workflow can be complex. However, as shown in this work, it is not only a tool to “see” phenomena, but also to measure up to a certain level of confidence. The experimental setup in this case does not involve a previous sample treatment, but also requires a good level of knowledge. Specifically, the use of external lighting, camera resolution and a correct focus of the region of interest are some of the variables which greatly determine the quality of the results, as shown in this work.

ACKNOWLEDGMENTS

The authors would like to acknowledge the support of the European Commission Horizon 2020 project Built2Spec (637221) and Science Foundation Ireland through the National Centre for Marine and Renewable Energy Ireland (MaREI) (Grant no. 12/RC/2302). The third author would also like to acknowledge the financial support of the Irish Research Council through a postgraduate fellowship. The last author would also like to acknowledge the support of Science Foundation Ireland through the Career Development Award programme (Grant no. 13/CDA/2200).

REFERENCES

[1]- McCormick, N., Lord, J., 2010. *Digital Image Correlation.* Materialstoday, vol 13, p 52-54.

[2] Grant, B., Stone, H., Withers, P.J., Preuss, M., 2009. *High-temperature strain field measurement using digital image correlation.* Journal of Strain Analysis for Engineering Design, vol 44, p 263-271.

[3] Wang, K., Carsley, J., He, B., Li, J., Zhang, L., 2014. *Measuring forming limit strains with digital image correlation analysis.* Journal of Materials Processing Technology, vol 214, p 1120-1130.

[4] Obreschkow, D., Kobel, P., Dorsaz, N., de Bosset, A., Nicollier, C., Farhat, M., 2006. *Cavitation Bubble Dynamics inside Liquid Drops in Microgravity*. Physical Review Letters, PRL 97.

[5] Kravtsova, A., Markovich, D.M., Pervunin, K.S., Timoshevsky, M.V., Hanjalic, K., 2013. *High-speed imaging of cavitation regimes on a round leading-edge flat plate and NACA0015 hydrofoil*. Journal of Visualization, vol 16:181-184.

[6] Lecompte, D., Smits, A., Bossuyt, S., Sol, H., Vantomme, J., Van Hemlrijck, D., Habraken, A.M., 2006. *Quality assessment of speckle patterns for digital image correlation*. Optics and Lasers in Engineering, vol 44, p 1132-1145.

[7] Crammond, G., Boyd, S.W., Dulieu-Barton, J.M., 2013. *Speckle pattern quality assessment for digital image correlation*. Optics and Lasers in Engineering, vol 51, p 1368-1378.

[8] Sun Yaofeng, Pang, J., 2007. *Study of optimal subset size in digital image correlation of speckle pattern image*s. Optics and lasers in engineering.